Techno-Science Research Journal 10(1) (2022) 45-56

Content list available at ITC

Techno-Science Research Journal

Journal Homepage: http://techno-srj.itc.edu.kh/

Techno-Science Research Journal

Flow Alteration under Land Use Impact in Sen River Basin of the Tonle Sap Lake Basin

Dydarong Ket[1], Ty Sok[1,2 *], Ilan Ich[1], Kimleang Chum[1,3], Sovatey Lim[1,3], Ratboren Chan[1,2], Ponleu Pech[1], Chantha Oeurng[1]

[1] *Faculty of Hydrology and Water Resources Engineering, Institute of Technology of Cambodia, Russian Federation Blvd., P.O. Box 86, Phnom Penh, Cambodia*

[2] *Research and Innovation Center, Institute of Technology of Cambodia, Phnom Penh, Cambodia*

[3] *College of Environment, Hohai University, Nanjing, Jiangsu, China*

Received: 20 January 2022; Accepted: 31 March 2022; Available online: June 2022

Abstract: *The expansion of agricultural land, especially for commercial crops, and deforestation caused by ever-increasing domestic and social-economic development have influenced the streamflow and altered water resources in the Sen River, one of the largest tributaries of the Tonle Sap Lake in Cambodia. The objective of this study was to examine the streamflow under land use change by using Supervised Land Use Maps generated from satellite images. Landsat 7 (ETM+) images for year 2009 and Landsat 8 (OLI) images for year 2015 and year 2020 were supervised classification to extract information on changes in land use by using ArcGIS 10.4.1 interface version. In this study, SWAT (Soil Water Assessment Tool) hydrological model is used to determine the effect of land use change on hydrological alteration in the Sen River Basin. The results showed that the SWAT model adjusted very well to the basin based on calibration and validation results. For land use change, most parts of the forest land were converted into agricultural land between 2009 and 2020, increasing by 14% (2009-2015), 33.5% (2015-2020) and 47% (2009-2020). In addition, it was observed that the land use changes led to increasing in 1-day, 3-day, 7-day, 30-day, and 90-day maximum and minimum flows. The monthly flows under land use changes ranged between -2% and 23%, which the increase of flow changes mostly occurred in the dry season. Based on these modeling results, the conversion of forest land to agricultural land was recognized as most LULC changes occurred, increasing streamflow, the risk of flooding and drought. This study could be beneficial to understand the effects of LULC change on the streamflow and help improve flood and drought control and water resource management planning in the Sen River Basin.*

Keywords: Flow alteration, Land use change, Supervised Land Use Maps, Sen River Basin, SWAT model

1. INTRODUCTION

The Tonle Sap Lake in Cambodia is the largest natural freshwater lake in Southeast Asia, and it is situated almost in the center of Cambodia and surrounded by five provinces such as Kampong Thom, Siem Reap, Battambang, Pursat, and Kampong Chhnang. As Cambodia's largest freshwater lake, it has played an important role in the country's economic, cultural, and environmental growth. Tonle Sap Lake is surrounded by 11 major tributaries and subbasins that flow into it. The region leading to runoff varies seasonally due to the normal season of subbasins in each catchment [1] . Global environmental change is both a cause and a result of land change. It has been identified as having significant implications for global and regional climates, global biogeochemical cycles such as carbon, nitrogen, water, biodiversity, and so on [2]. As the global population and per capita consumption rise, so makes the demand for food, natural resources, and the ecosystem is stressed [3]. Variations in vegetation stomatal conductance, surface roughness, hydraulic connectivity, and other soil properties such as organic material, composition, and infiltration rate are all affected by land use change at the catchment level [4].

Forest cover in Cambodia during 1998 was considered in the highest levels in Southeast Asia, nowadays the acceleration is appeared over the last few decades due to the pace of land use

* Corresponding author: Ty Sok
E-mail: sokty@itc.edu.kh; Tel: +855-11 980 698

and forest conservation [5]. In 1970s, forest covered an estimated

73% of the country territory [6]. To monitor the loss of forest land, forest cover assessment was conducted in 2016, which shows the result of land cover changes to 48% of the total area of Cambodia [5]. In most countries, the loss of forest cover corresponds to land use and land cover change trends linked with demographic increase and economic development [7]. The population of Cambodia has been steadily increasing. The population has increased from roughly 3 million in 1980 to about 13.4 million in 2008 and has continuously risen to about 15.3 million in 2019, which grows 14.1% in 11 years between 2008 and 2019 [8]. About 2-3 million people reside in cities, while the remainder lives in rural regions and rely on natural resources, particularly forest and non-forest goods, to get around. Due to their demands for areas for settlement and agriculture, this large population growth rate may result in greater deforestation [6]. Agriculture is one of Cambodia's most important industries, which provided for 33.5 percent of the country's GDP in 2009 and employed 56 percent of the workforce [9]. In Cambodia, water is the most important natural resource for long-term development and poverty reduction, such as irrigated agriculture which consumes a large amount of fresh water and often creates water scarcity.

The availability and quality of water resources are thought to be affected by land use activities. These effects can be both beneficial and detrimental. It seems intuitive that the benefits of effective land management, or the costs associated with negative impacts of insufficient land use on water resources, should be felt not only by the water users who cause them but also by those who live downstream or, in the case of groundwater, use the affected groundwater resources [10]. To measure these costs and benefits, it's necessary to get a clear picture of how different land use activities affect hydrologic regime and water quality from a landscape perspective, as well as at what watershed scale the impacts are important. Land use effects on water quality are influenced by a variety of environmental and socio-economic factors. Climate, topography, and soil composition are all-natural factors. Economic capacity and knowledge of farmers, management practices, and the growth of infrastructure, such as roads, are all socio-economic factors. Furthermore, agricultural land use effects can be difficult to discern from natural or other human impacts, such as the effect of agricultural runoff versus rural sewage systems on surface and groundwater depletion. Impacts on surface water supplies and groundwater resources can be differentiated when it comes to the hydrologic regime. Impacts on peak flows and impacts on dry season flows are important factors in the above case. In terms of groundwater, the effect of land use on groundwater recharge must be investigated [10,11]. The most important factor of the effect of land use on mean runoff is the plant cover's water regime in terms of evapotranspiration (ET), the soil's ability to retain water (infiltration capacity), and the plant cover's ability to intercept moisture resulting a significant influence on runoff characteristics and groundwater in the basin [12]. It may also alter meteorological parameters by changing surface temperature, increasing evaporation, and reducing transpiration rates, which has discovered that forest cover and water yield have a strong positive correlation [13]. A study in northwest China found that mean annual runoff declined by 2.3% regarding a 25% increase in the proportion of forest land in a basin [14]. An increase of streamflow from 0.2 to 0.4% was associated with a decline of 16.3% in the forest land of a river catchment in Vietnam [15].

In order to address the above problem, it is essential to have a good understanding of the causes and consequences of the overall hydrologic regime and the historical trend of land use change by using hydrological knowledge with practical and effective methods. Hydrological models are a useful tool to simulate the rainfall-runoff process in different time space associated for better understanding of the hydrological process and streamflow generation of a catchment. The aim of this study was to analyze the flow alteration under land use impact in Sen River Basin by calculating dynamic land use map in 2009, 2015, and 2020 generated from satellite images using Supervised Land Use Maps in ArcGIS. Furthermore, the daily flow calibration and validation was performed in SWAT model and then, the simulated flow from three land use maps was evaluated by using Indicator of Hydrologic Alteration (IHA).

2. METHODOLOGY

2.1 Sen River Basin, the largest tributary of Tonle Sap basin

Sen River Basin is the largest tributary of the greatest lake which covers a part of Preah Vihear Province and Kampong Thom Province of Cambodia, and the study area on this river covers approximately 16,000 km^2 with 520 km length from the boundary of north Cambodia to the ends at Tonle Sap Lake. The river has lied between 12°30′ N to 14°30’ N of latitudes and 104°00’ to 105°30’ E of longitudes (Fig.1). Sen River Basin originates in the mountainous chains of Dangrek in Preah Vihear Province from the maximum altitude of around 790 m and flows into Tonle Sap Lake via the district of Stung Sen, Kampong Thom Province, which is located in the center part of Cambodia. With a standard deviation of 320 m^3/s, the mean flow of the Sen River is 249 m^3/s [16]. The Sen River's average annual precipitation is 1,400 mm, discharging approximately 325 m^3/s to Tonle Sap Lake [17]. Tropical monsoons with two distinct seasons dominate the climate in the Stung Sen basin. The rainy season is between May and October, and the dry season is between November and April. The average annual rainfall is about 1,500 mm, and with maximum and minimum temperatures 35ºC and 20ºC, the average temperature is around 27.5ºC [18]. In this period, the annual rainfall is concentrated, producing annual precipitation of around 1,400 mm per year [19]. It has been assessed that the Sen River Basin has the most plentiful water supplies and important hydropower capacity in Cambodia.

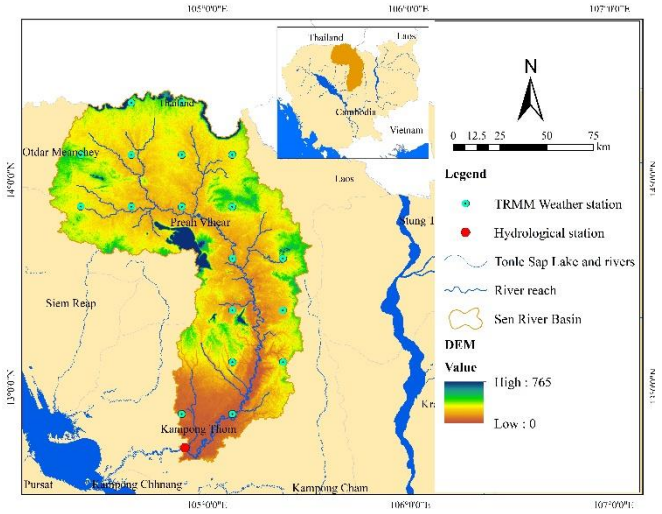

Fig. 1. Location of the study area in Sen River Basin

2.2 Model description

The Soil and Water Assessment Tool (SWAT) was developed by Dr Jeff Arnold for the USDA Agricultural Research Service. SWAT is used to simulate the catchment runoff and land management process, which allow the watershed to be divided into subbasins with one stream containing each based on the data estimation of soils classification, land use, daily rainfall and topography [20]. The software package of SWAT is worked as facilities to predict the impact of watersheds from land management, sediment and agricultural chemical yields, land use and simulate hydrologic cycle and root growth of the plant and can specify the region of water routing to major river basins over the long periods [21]. Hydrologic response units (HRUs) are areas in which soil type, land use, land slope have a unique combination to be spatially disconnected by regions with no designated geographic location [22]. A previous study related to irrigation of the Del Reguero watershed in Spain showed the established result of using the SWAT model to assess the impact of non-point phosphorus losses with various management practices. Water quantity and quality data (2008 to 2009) and field surveys were recorded and inputted for performing calibration and validation [23]. In California, the San Joaquin watershed that depends on irrigation met the climate change and increasing of variation of atmospheric CO_2 was using the modelling of SWAT to response these issues and as the result of modelling shown the significant effects on water yield, irrigation water use, stream flow and evapotranspiration which indicated that this watershed is sensitively on potential of future climate change [24] .

Water balance is the important force in the process of the watershed model in the hydrologic cycle simulation of SWAT, which includes evapotranspiration, rainfall, percolation, surface runoff, lateral flow, infiltration, lateral flow, and groundwater up flux [22]. Hydrology simulation of a watershed is separated into two phases such as the land phase and the water or routing phase. The land phase of the hydrologic cycle inspects the amount of water, nutrient, pesticide loading and sediment to the main channel of each subbasin and the water phase specifies the movement of water, sediments in the hydrologic cycle of the basin. The water balance equation, which is shown in Eq. 1, can be simulated in the hydrologic cycle [20].

$$SW_t = SW_o + \sum_{i=1}^{t}\left(R_{day} - Q_{surf} - E_a - w_{seep} - Q_{gw}\right) \quad \text{(Eq. 1)}$$

where:

SW_t = the final soil water content (mm)

SW_o = the initial soil water content on day i (mm)

t = the time (days)

R_{day} = the amount of precipitation on day i (mm)

Q_{surf} = the amount of surface runoff on day i (mm)

E_a = the amount of evapotranspiration on day i (mm)

w_{seep} = the amount of water entering the vadose zone from the soil profile on day i (mm)

Q_{gw} = the amount of return flow on day I (mm).

There are two objectives for this study illustrating the SWAT Model Calibration and Validation for Objective 1 and Flow Alteration under Land use Change for Objective 2, which is shown in Fig.2. The SWAT-CUP was utilized for analyzing the sensitivity parameter and calibration. The interface of SWAT-CUP was developed for any uncertainty calibration using multiple regression to evaluate the sensitive parameters, which can easily be linked with SWAT. The Student's t-value distribution, which is a statistical distribution was used to get the statistic value (p-value) of each parameter [25]. For each term of parameters, the p-value checks the null hypothesis that each parameter 's coefficient is equal to zero (no effect). Sixteen parameters were selected to be used for sensitivity analysis by running 500 times in SWAT-CUP based on Student's t-test. Calibration is an attempt to better parameterize a model, conditionally reducing the variance of the forecast to a certain set of local parameters by carefully selecting the values for the model input parameters within their respective uncertainty ranges [26]. This method was used most sensitive model parameters that differentiated in SWAT-CUP for calibration process of the SWAT models. By selecting the period from 2001 to 2006 as sensitivity analysis period, the model calibration process was carried out for NSE at least 0.60. Model validation was performed using the calibrated parameters applied on the observed data in different period [26]. Data period of model validation process between 2006 and 2008 was conducted in SWAT interface in ArcGIS by changing parameters values.

In model performance and evaluation, Nash-Sutcliffe efficiency (NSE) is a statistical distribution indicating how well the plot of observed data versus simulated data fits the 1:1 line. NSE ranges from $-\infty$ to 1, with NSE = 1 being the optimal

value. The level performance is generally acceptable between the value of 0 and 1, whereas the negative value shows very poor and the average value of output is a better estimate than the model prediction. Regression (R^2) is a statistical measurement that shows how the simulation data fitted to the observed data which is known as the coefficient of determination or the coefficient of multiple determination for multiple regressions. The better prediction and estimation of model simulation is indicated by the higher R^2. RSR is an error index statistic standardizing Root Mean Square Error (RMSE) using standard deviation (STDEV). RSR varies from the optimal value of 0 indicating residual variation. If RSR is become lower, the model indicates better simulation performance.

1

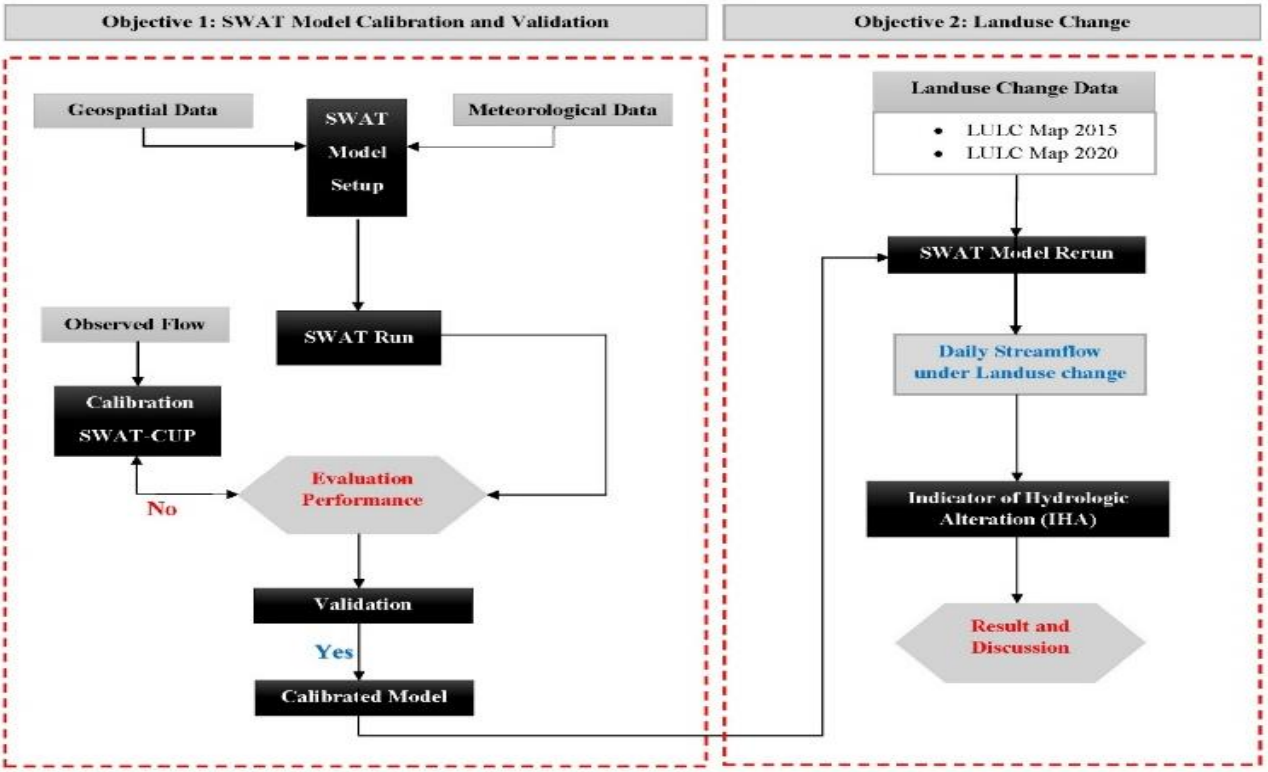

Fig. 2. The procedure of study for SWAT model calibration and validation and land use change

2.3 Indicator of hydrologic alteration (IHA)

The IHA was employed to evaluate the hydrologic alteration after the separating study period using the range of variability approach (RVA) with 33 hydrologic alteration parameters [27]. The 17 hydrologic parameters focus on the magnitude, duration, timing, and frequency of extreme events and geomorphology. At the same time, the other 16 parameters measure the central tendency of either the magnitude or rate of change of water condition. These 33 parameters were categorized into 5 groups addressing the magnitude, timing, frequency, duration, and rate of change. In this study, only group 1 and group 2 featuring magnitude, timing, and duration are utilized to evaluate the result of land use impact on streamflow in the basin.

2.4 Land use analysis

Applying LULC mapping is a critical issue for collecting information for master city planning and monitoring the environment. Any supervised classification does not complete until an assessment of its accuracy has been performed. Accuracy assessment is a quantification of estimation with the aid of remotely sensed dataset to classification conditions, and it is useful for evaluation of classification approach, and it is also important to determine the error that might be involved. The accuracy assessment of classification is proposed in the form confusion matrix [28]. In this study, the producer's accuracy (PA), the user's accuracy (UA), the overall accuracy and the Kappa Coefficient (K) are used to verify with reference sample data which produce error matrices generated from supervised images of the satellite.

The producer's accuracy (PA) is the number of correctly classified samples of a particular category divided by the total number of reference samples for that category. It is a measure of the error of omission [29]. The user's accuracy (UA) is an

alternative measure for individual category accuracy. It is the number of correctly classified samples of a particular category divided by the total number of samples being classified as that category. It measures the error of commission. The overall accuracy is the total number of correctly classified samples divided by the total number of samples. It measures the accuracy of the entire image without any indication of the accuracy of individual categories. The weight of each category depends on the number of samples in that category [30] . It has a tendency to be biased toward the category with a larger number of samples.

$$K = \frac{N\sum_{i=1}^{r} x_{ii} - \sum_{i=1}^{r}(x_{i+} \cdot x_{+i})}{N^2 - \sum_{i=1}^{r}(x_{i+} \cdot x_{+i})} \quad \text{(Eq. 2)}$$

where:

r = the number of rows in the error matrix

x_{ii} = the number of observations in row i and column i

$+$ = summation over the index

x_{i+} = the marginal totals of row i

x_{+i} = the marginal totals of column i

N = the total number of observations.

The Kappa coefficient (K) which shown in Eq. 2, is a measure of the actual agreement (indicated by the diagonal elements of the matrix) minus chance agreement (indicated by the product of row and column marginals). It uses all cells in the matrix and takes into account both the commission and omission errors [31]. Kappa value is computed for each error matrix. It measures how the classification performs as compared to the reference data.

2.5 Model input

For Sen River Basin, the SWAT model was used with geospatial data, meteorological data as key data input to obtain for running the model. The daily rainfall from the Tropical Rainfall Measuring Mission (TRMM) was located with 18 rainfall stations in the year 1998 to 2019. Temperature, humidity, wind speed and solar radiation data were collected in the basin and received from Global Weather for SWAT while land uses/land covers are classified with satellite images by ArcGIS with 4 classes, and soil types are conducted by Mekong River Commission (MRC) with 21 classes.

Climatological data such as temperature, humidity, wind speed and solar radiation were collected from Global weather data, and Daily rainfall from TRMM data (mirador.gsfc.nasa.gov). 18 Stations across the basin were considered for rainfall-runoff based on data availability for the year 1998-2019 shown in Fig.1. The missing climatological data were filled in from the nearby station based on their correlation. The simulation of streamflow utilizes daily rainfall data between 1998 and 2008. The lowest capacity of monthly rainfall in Stung Sen River was in January, while in August, monthly rainfall reached the peak, which is shown in Fig.3.

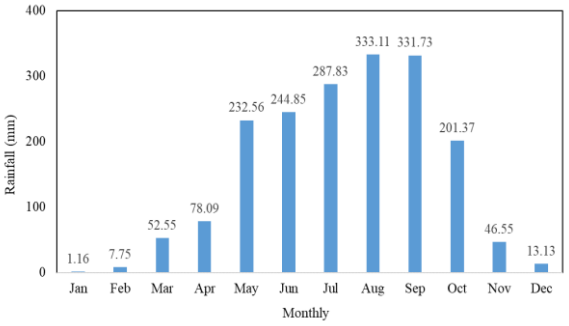

Fig. 3. Average monthly rainfall from 14 stations in Sen River Basin

The hydrological station is located in Kampong Thom province. Observed discharge, measured between 1st January 2001 and 31st December 2008 in this hydrological station, was obtained from the Department of Hydrology and River Work of Ministry of Water Resources and Meteorology. The daily observed streamflow is shown in Fig.4 were examined and compared from 2001 to 2008. The streamflow reached the peak to considerably less than 800 m^3/s in 2002 during the rainy season.

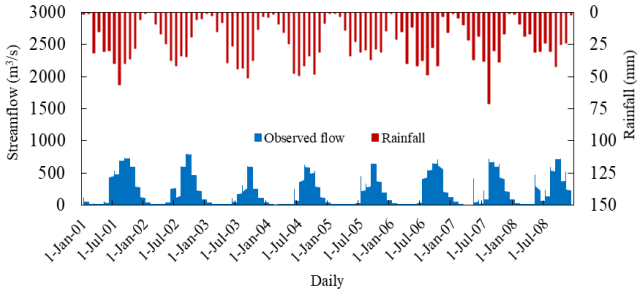

Fig. 4. Rainfall and average daily observed flow of Sen River Basin

The images with 30 m resolution and no cloud cover were collected from U.S Geological Survey (USGS) Center for Earth Resources Observation and Science (EROS) (https://earthexplorer.usgs.gov), which is shown in Fig.1. Land use map was generated using Landsat 7 (ETM+) for 2009, Landsat 8 (OLI) for 2015 and 2020 land use map images and supervised classification using ArcGIS 10.4.1 with 4 categorized classes such as forest land, agriculture land, bareland, and water which is shown in Fig.5. Two hundred fifty random points were produced as accuracy assessment points in ArcGIS to perform using reference data obtained from the interpretation of corresponding high-resolution Google Earth Images of 2009, 2015, and 2020 to illustrate the representativeness of the classified images on the ground. Supervised land use map 2009 is used as the baseline of study with most part of this area covered by Forest land is 11,517 km^2,

equal to 81% of the total basin and the most second part, which is about 9.41% for bareland. Agriculture is covered 9% of the area, and water spreads only 0.4% around the basin.

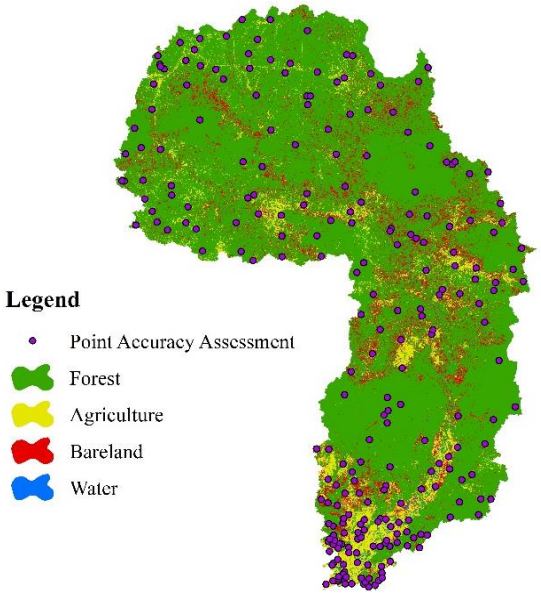

Fig. 5. Classification of supervised land use 2009 for SWAT model in Sen River Basin

There are 21 different soil types from MRC are covered in the basin area, which is shown in Fig.6. Most of the region is covered by Haplic Acrisol/Dystric Leptosol 19.56% and some other parts of the basin while Luvic Arenosol (ARl/ARh) 30.66% covered on the northeast of the basin, Leyic Acrisol/Plinthic Acrisol (ACg/ACp) 15.08% on the west and other soil types have lied from northeast to the main outlet of the basin [32]. These types of soils provide shallow potential rooting depth, high groundwater tables, and high bulk density for the basin.

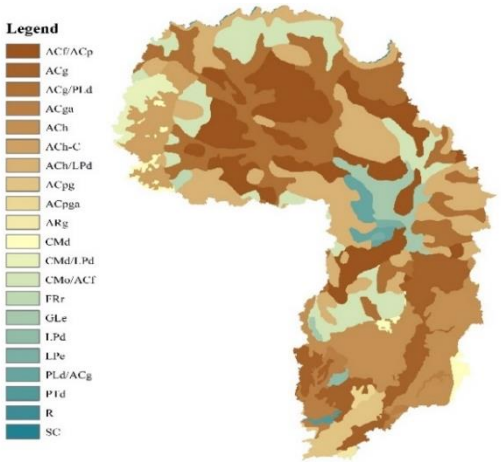

Fig. 6. Classification of supervised land use 2009 for SWAT model in Sen River Basin

3. RESULTS AND DISCUSSION

3.1 Land use classification and change detection

Four land use categories, namely forest land, agriculture land, bareland, and water are indicated. Landsat 7 (ETM+) was used to generate LULC maps in 2009, and Landsat 8 (OLI) was used to create LULC maps in 2015 and 2020 (Fig.7). Table 1, Table 2, and Table 3 provide the accuracy reports for the four classified images. The producer's accuracy (PA) and the user's accuracy (UA) showed higher percentage of each land use classification. For the years 2009, 2015, and 2020, the overall accuracy ranged from 88% to 97%. The four classified images all obtained a Kappa coefficient of at least 0.80, which are very good indicators of classified images. Therefore, the validation data set indicated a very good agreement with the classified image. According to Landsat image analysis, agriculture land rose by 14% between 2009 and 2015, whereas other land covers decreased forest land (9%), bareland (5%), and water (0.20%) particularly. Agriculture land had a higher than other land cover categories during the research period, and it steadily expanded between years. As a result, agriculture land was the most common land cover contributing to 9% in 2009, 22% in 2015, and 56% in 2020, while forest land coverage at 81% in 2009, 72% in 2015, 38% in 2020. Bareland was the third most common land cover in 2009 with 9%, 5% in 2015, and 6% in 2020. Water cover percentages ranged from 0.40% in 2009 to 0.20% in 2015, and 0.13% in 2020. This rapid growth of urbanization, and policy change [33].

Table 1 Confusion matrix of 2009 land use classification

2009 LULC Class	F	A	B	W	Total User	UA (%)
F	144	2	0	1	147	97.96
A	2	38	5	2	47	80.85
B	10	3	17	1	31	54.84
W	2	0	0	23	25	92
Total Producer	158	43	22	27	250	81.41
PA (%)	91.14	88.37	77.27	85.19	85.49	83.45

(F) Forest, (A) Agriculture, (B) Bareland, (W) Water
Overall accuracy = 88.80%; Kappa Statistic = 0.80

3.2 Model calibration and validation

As shown in Fig.8 and Table 4, the calibration periods (2001 to 2006) and the validation period (2006 to 2008), the NSE values were 0.70 and 0.76, and the RSR values which were 0.55 and 0.49, respectively. The R^2 values were 0.81 for both calibration and validation.

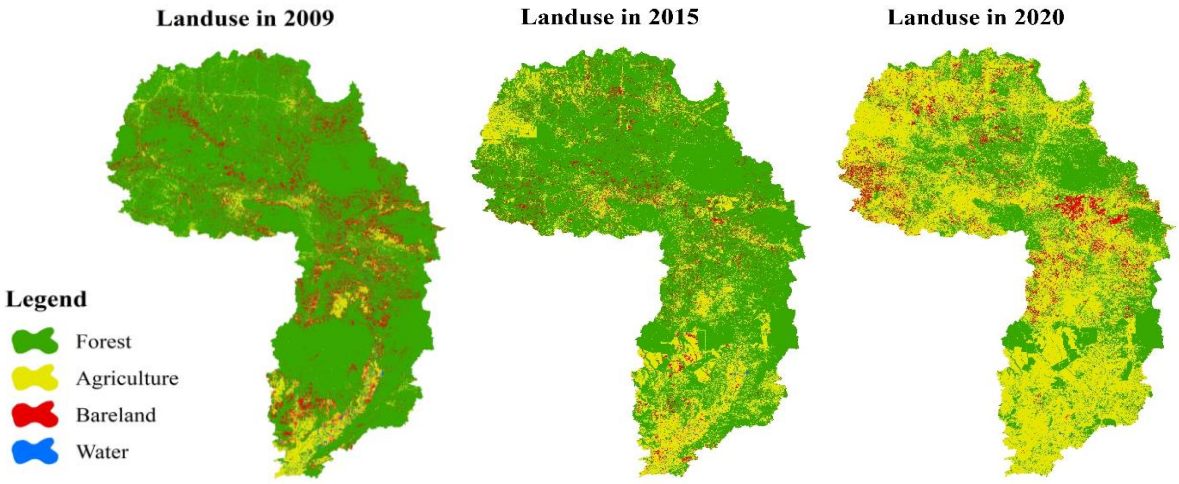

Fig. 7. Land use classification of Sen River Basin (2009, 2015, and 2020)

Table 2 Confusion matrix of 2015 land use classification

2015 LULC Class	F	A	B	W	Total User	UA (%)
F	99	3	1	0	103	96.12
A	2	59	1	0	62	95.16
B	1	7	40	1	49	81.63
W	1	0	0	354	36	97.22
Total Producer	103	69	42	36	250	92.53
PA (%)	96.12	85.51	95.24	97.22	93.52	93.03

Overall accuracy = 93.20%; Kappa Statistic = 0.90

Table 3 Confusion matrix of 2020 land use classification

2020 LULC Class	F	A	B	W	Total User	UA (%)
F	74	1	0	0	75	98.67
A	4	96	2	0	102	94.12
B	0	2	25	0	27	92.59
W	0	0	0	46	46	100
Total Producer	78	99	27	46	250	96.36
PA (%)	94.87	96.97	92.59	100	96.11	96.23

Overall accuracy = 96.40%; Kappa Statistic = 0.85

As a result, NSE and RSR values suggest that the model showed a good performance and a very good statistical range between simulated and observed during the calibration and validation period, respectively, while R^2 values suggest that the model showed very good performances. The statistic value outcomes of the calibration of the streamflow are consistent with the observed flow. The overall performance of the model calibration and validation replicated the observed flow for an independent dataset reasonably well.

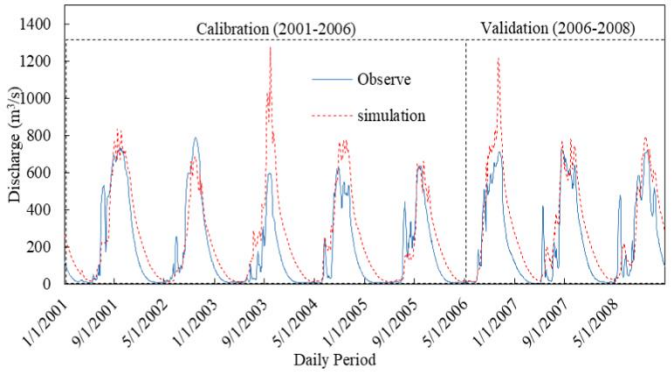

Fig. 8. Daily streamflow evaluation of model calibration and validation period in Sen River Basin

3.3 Impact of land use change on streamflow

As shown in Fig.9, a comparison between the streamflow of the Sen River Basin simulated from LULC maps of 2009, 2015, and 2020 obtained differences in flow discharges which indicated that the observed change of LULC has a significant impact on streamflow in all sub-basin under the same climatic input. Overall, the streamflow under 3 LULC increased with a slight change of simulated result between different land uses from May until September during seasonal rainfall before declining in October of baseline LULC 2009 while continuously started to rise for simulated streamflow of LULC 2015 and

LULC 2020 and went down during the dry season. At the beginning of the rainy season, streamflow was between 44 to 52 m^3/s for each LULC.

Table 4 Statistical performance of calibration and validation for daily streamflow of Sen River Basin

Statistical Indicator	Calibration	Per. Rating	Validation	Per. Rating
NSE	0.70	Good	0.76	Very Good
R^2	0.81	Very Good	0.81	Very Good
RSR	0.55	Good	0.49	Very Good

Over the following 5 months of the rainy season, the streamflow of 3 LULCs was almost the same before the flow of baseline reached the peak at 638 m^3/s in September. October saw the highest results of flow under LULC 2015 and LULC 2020 by 638 m^3/s and 657 m^3/s, respectively. In the dry season, there is a different change of streamflow between the three LULCs during the period with the increase of flow under LULC 2015 and LULC 2020 compared to the streamflow of the baseline LULC map. However, these 3 flows of LULC fell to around 43 to 51 m^3/s towards the end of the dry season. Therefore, according to the result from Fig.7, the trend of flow increasing is during the dry season due to the extent of agriculture area over forest land from 2009 till 2020 [34].

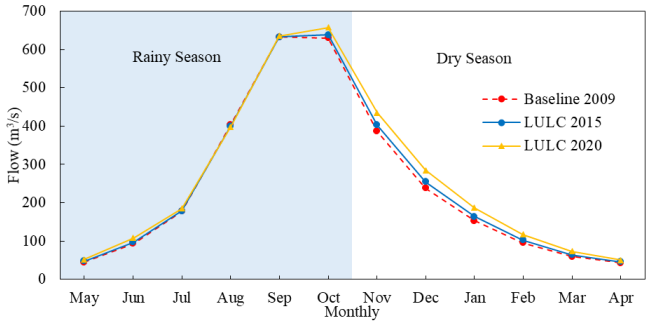

Fig. 9. Monthly flow change of land use 2009, 2015, and 2020

The flow changes have resulted from the simulation of three different LULC maps of Sen River Basin. Fig.10 indicated the change of average monthly streamflow that occurred between 2009 and 2020. Three graphs of flow change, such as flow change from 2009 to 2015, 2009 to 2020, and 2015 to 2020, are shown with quantity change and percentage change of streamflow. Over the period of land use change, the monthly flow from October till July has remained increasing, then seem

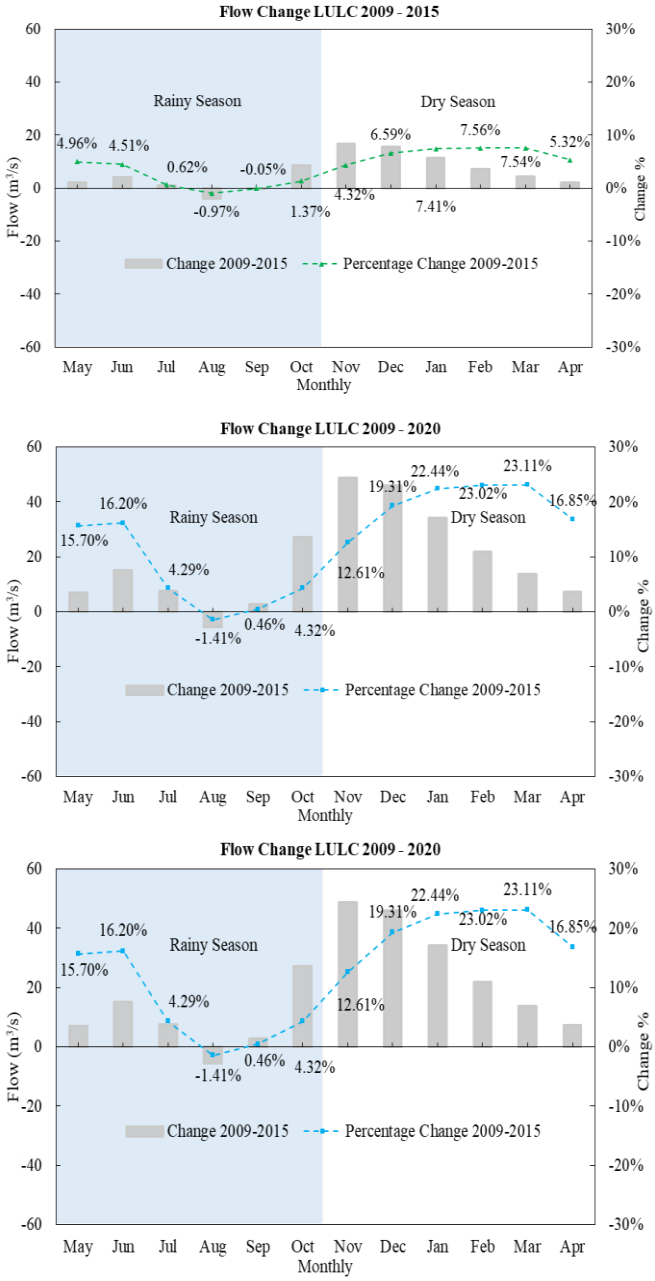

Fig. 10. Comparison in value of flow change and percentage change from 2009 to 2015, 2009 to 2020, and 2015 to 2020

a decrease of streamflow in August. In September, the monthly flow between 2009 and 2015 has decreased and then started to rise from 2015 to 2020. As with the change of LULC 2009 to 2015 and LULC 2015 to 2020, the average peak of flow over the whole basin was at 8% in February and 14% in March, respectively, while bottoming out with the percentage of -0.97 and – 0.45 in August. Most flow changes during 2015 to 2020 exhibited a doubled pattern compared to flow change during

2009 to 2015. The flow under LULC change over 12 years was ranged between -1% and 24%. Overall, the increase of flow changes mostly occurred in the dry season due to the deforestation in the study area and transformed to cropland cover, which affect the water cycle and runoff. Because shallower-rooted plants cannot access deep soil water during dry periods, the magnitude of ET and its seasonal pattern are altered as a result of the transition from deep-rooted forest to shallower-rooted plants, resulting in higher streamflow [35].

3.4 Impact of land use change on multiple temporal scales

Daily minimum and maximum flows of the simulated period were considered in Figs.11 and 12. In the minimum flow, the simulated flow in 2007 rises to the highest value of all LULC study periods except the 30-day condition, which peaked in 2008. All results in minimum daily flow show the lowest point for LULC 2009, followed by the flow of LULC 2015. Conversely, in maximum daily flow, the peaked flow fluctuated on different LULC period maps at the different conditions of flow in the 2007 simulation period while the 1-day maximum peaked in 2003 simulated period. The maximum daily flow of LULC 2009 indicates the lowest value for all period conditions. Overall, the alteration of minimum flow conditions shows not differ greatly, except in 90-minimum flow condition shows a dramatic change compared to other, while in annual maximum flow conditions illustrate the decreasing of flow from 1-day till 90- day condition.

Fig.13 illustrates the average streamflow of LULC in 3 different periods and the change of flow streamflow from one period to another over the extreme annual condition. This will be focused on minimums and maximums of streamflow on 1-, 3-, 7-, 30-, and 90-days. All simulated flows reach the maximum and the minimum in 1-day condition, and the highest change is likely in 90-day minimum condition while the lowest percentage of flow change is in 1-day maximum condition. The mean flow of LULC 2020 received the highest streamflow of all annual minimum conditions, while the mean flow of LULC 2009 is given the lowest result. On the other hand, in annual maximum condition, LULC 2009 receives the highest in 1-, 3-, and 7-day conditions, whereas 30- and 90-day conditions show in LULC 2020. The change over 12 years of study increases to the maximum of 17% and decreases to the minimum of 1.6%. The comparison of the flow change in each extreme condition from 3 land use maps reveals not differ significantly from time to time which may be the result from the change in water components including surface runoff, lateral flow, groundwater recharge that would affect flow in the whole basin rather than the flow at the outlet. Detection of flow may show the change at different locations of the outlet due to land use change is spatial. The impact of water allocation for agriculture and other factors in each season and climate change in the basin during the period of study may also contribute as the driver in these differences. The change in minimum flow is high since the value of minimum is small (from 20 m^3/s), thus the small change can lead to high percentage change.

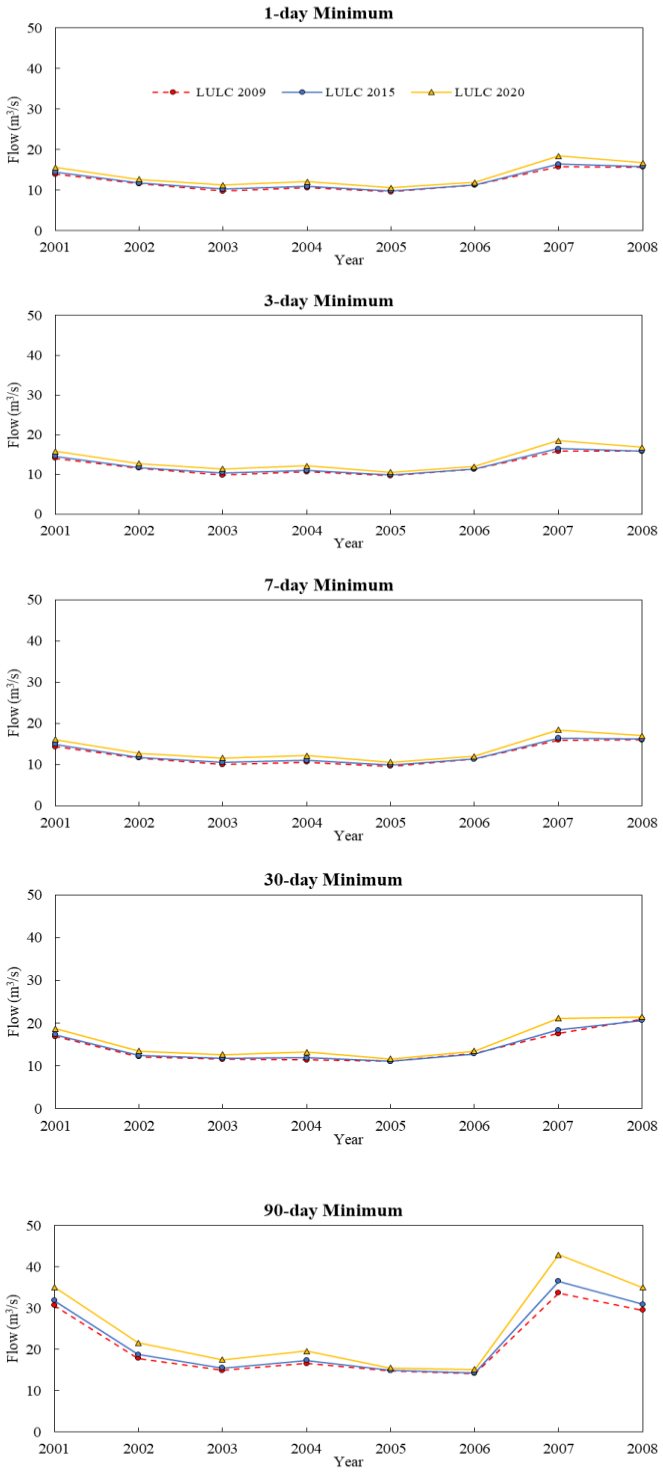

Fig. 11. Comparison of annual 1-day minimum, 3-day minimum, 7-day minimum, 30-day minimum, and 90-day Minimum Condition of Streamflow for Land use 2009, 2015, and 2020 in Sen River Basin

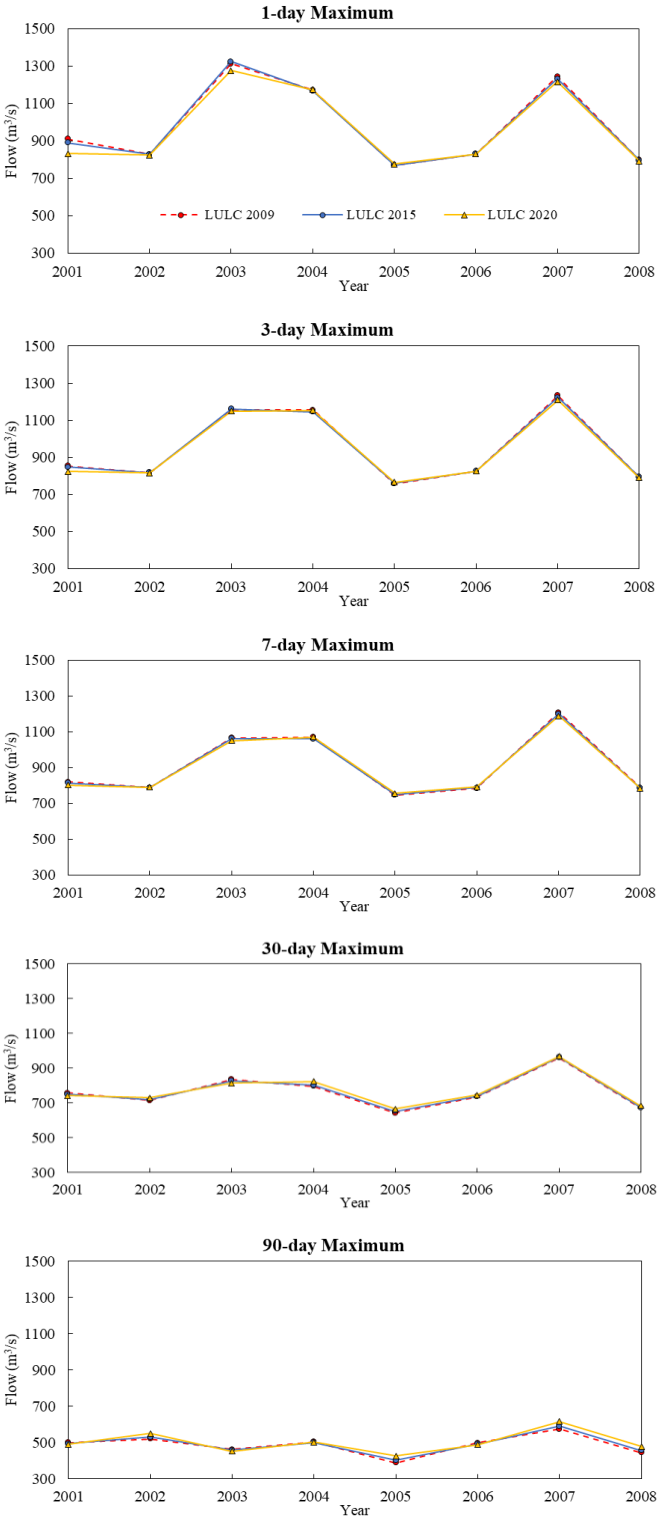

Fig.12. Comparison of annual 1-day maximum, 3-day maximum, 7-day maximum, 30-day maximum, and 90-day maximum condition of streamflow for land use 2009, 2015, and 2020 in Sen River Basin

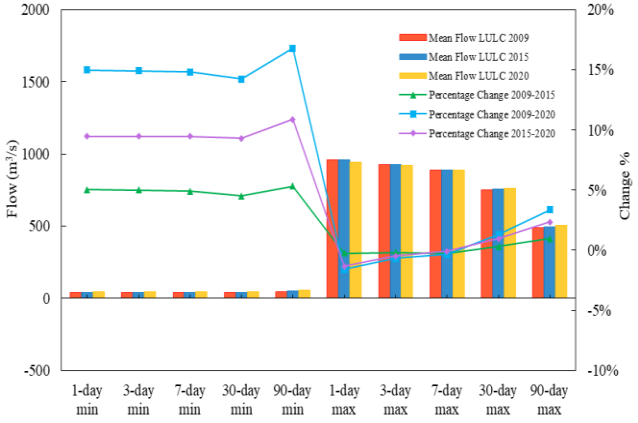

Fig.13. Average streamflow and percentage change in minimum and maximum of time condition for land use 2009, 2015, and 2020 in Sen River Basin

3.5 Impact of Land Use Change on Flow Duration Curve

Flow duration curve is characterized into different segments by percentage exceeded, which is shown in Fig.14. The first segment from 0 to 10% of flow exceedance describes high flows, the second part (10-40%) represents wet conditions, 40 to 60% shows mid-ranges flows, another segment between 60% and 90% gives dry condition, and another partition represents long-term streamflow sustainability. The peaked curve indicates the discharge of 1313 m^3/s, 1324 m^3/s, and 1277 m^3/s for the LULC 2009, LULC 2015, and LULC 2020, respectively. The average flow of 495 m^3/s of LULC 2009, 502 m^3/s of LULC 2009 and 523 m^3/s of LULC 2020 surpassed 20 percent exceedance. The LULC 2009 reveals that 15 m^3/s is equaled or exceeded 90% of the time in the low flow zone while LULC 2015 shows 16 m^3/s, whereas 17 m^3/s is equaled or surpassed 90% of the LULC 2020. Overall, the highest flow among these flow duration curves is in LULC 2015, while in wet and dry conditions, the flow duration curve of LULC 2020 reaches the highest.

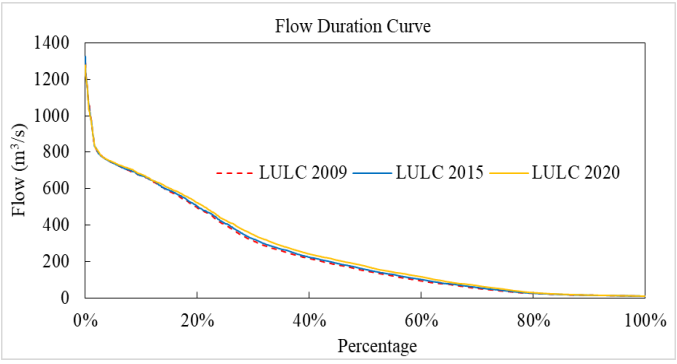

Fig.14. Flow duration curve under land use of 2009, 2015, and 2020 in Sen River Basin

The low flows were proportionally more affected than high flows due to low flow affected by changes in transpiration, while high flow is affected by changes in interception and transpiration. The decreased of forest land in the basin is likely to reduce the rates of interception and transpiration, thus having higher flow.

4. CONCLUSIONS

This study determined the possible effects of land use changes on the hydrologic regime alteration in the Sen River Basin. The set-up SWAT model for analyzing the effect of land use change in the Sen River Basin was considered to have the capacity of representing the watershed properly.

The findings revealed that the land use/land cover in the Sen River Basin had changed dramatically over the last 12 years. The major land use activity in the entire watershed and some watersheds, in particular, was deforestation and subsequent expansion of agricultural land [36,37]. Forest land was converted to agriculture land from year to year and there was also a decrease in bareland. There was also a decrease in bareland. The result has shown that the magnitude of agriculture land was increased by 14% from 2009 to 2015, by 33% from 2015 to 2020 and by 48% from 2009 to 2020, which entirely affected the watershed hydrology in the study area.

Generally, streamflow has shown an increase from time to time by using three different dynamic LULC maps generated from satellite images in 2009, 2015, and 2020, and result illustrated as average monthly flows, annual maximum and minimum condition of streamflow, and percentage change of streamflow using simulated streamflow from 3 different periods of LULC map in SWAT model. The main reason behind these changes of streamflow over the period is the relationship of forest land and agriculture land with the hydrologic cycle [38]. Soils in forests function like sponges, retaining water for longer periods of time than soils in other land uses [39] . Based on the conversion of forest land to agriculture land was recognized as most LULC changes occurred, which could increase water discharge, the risk of flooding and drought in the basin. According to the results, if the deforestation and expansion of agriculture land trends are allowed to continue, the hydrologic cycle in this basin will be affected, which will result in an increase in streamflow in the basin. Understanding these impacts can improve future land use planning and water resource management in the basin by regulating the proper land use to maintain the hydrological balance.

ACKNOWLEDGMENTS

The study was supported and funded by SUMERNET4 All Joint Action Project for strengthening flood risk management caused by climate change in Stung Sen River Basin, Cambodia (FloodCam). The authors would also like to thank the Ministry of Water Resources and Meteorology (MOWRAM) of Cambodia for providing the data for this study.

REFERENCES

[1] Surface Processes and Landforms, 1865(April), 1855–1865.

[2] Goldewijk, K. K., & Ramankutty, N. (2004). Land cover change over the last three centuries due to human activities : The availability of new global data sets. GeoJournal, 335–344.

[3] Song, X., Hansen, M. C., Stephen, V., Peter, V., Tyukavina, A., Vermote, E. F., & Townshend, J. R. (2018). Global land change from 1982 to 2016. Nature Research, 16.

[4] Fiener, P., Auerswald, K., & Oost, K. Van. (2011). Earth-Science Reviews Spatio-temporal patterns in land use and management affecting surface runoff response of agricultural catchments — A review. Earth Science Reviews, 106(1–2), 92–104.

[5] MOE. (2018). Cambodia Forest Cover 2016 (Issue March). The Ministry of Environment of Cambodia.

[6] FA. (2008). Kingdom of Cambodia Country Paper on Forestry Outlook 2020. Forestry Administration, Cambodia, June, 1–37.

[7] FA. (2010). Cambodia Forestry Outlook Study. Food and Agriculture Organizaion of the United Nations, 39.

[8] NIS. (2019). General Population Census of the Kingdom of Cambodia 2019. In Ministry of Planning (Vol. 53, Issue June 2019).

[9] TONG Kimsun, H. S. & P. S. (2011). What limits agriculture intensification in Cambodia? The role of emigration, agriculture extension services and credit constraints. Cambodia's Leading Independent Development Policy Research Institute (CDRI), 7, 1–4.

[10] Kiersch, B., & Division, W. D. (2000). Land-Water Linkages in Rural Watersheds Electronic Workshop A literature review. Food and Agriculture Organizaion of the United Nations, 1, 12.

[11] Hasan, S. S., Zhen, L., Miah, M. G., Ahamed, T., & Samie, A. (2020). Impact of land use change on ecosystem services: A review. Environmental Development, 34(April).

[12] Foley, J. A., DeFries, R., Asner, G. P., Barford, C., Bonan, G., Carpenter, S. R., Chapin, F. S., Coe, M. T., Daily, G. C., Gibbs, H. K., Helkowski, J. H., Holloway, T., Howard, E. A., Kucharik, C. J., Monfreda, C., Patz, J. A., Prentice, I. C., Ramankutty, N., & Snyder, P. K. (2005). Global consequences of land use. Science, 309(5734), 570–574.

[13] Vertessy, R. A., Watson, F. G. R., O'Sullivan, S. K., Davis, S. H., xCampbell, R., Benyon, R. J., & Haydon, S. R. (1998). Predicting water yield from mountain ash forest catchments. In Industry Report No. 98/4.

[14] Cooper, M. (2010). Advanced Bash-Scripting Guide An in-depth exploration of the art of shell scripting Table of Contents. Hydrological Processes, 2274(November 2008), 2267–2274.

[15] Khoi, D. N., & Thom, V. T. (2015). Parameter uncertainty analysis for simulating streamflow in a river catchment of Vietnam. Global Ecology and Conservation, 4, 538–548.

[16] Theara, T., Sarit, C., & Chantha, O. (2020). Integrated modeling to assess flow changes due to future dam development and operation in stung sen river of tonle Sap Lake Basin, Cambodia. Journal of Water and Climate Change, 11(4), 1123–1133.

[17] Marith, M., Weerakoon, S. B., Sokchhay, H., & Chantha, O. (2016). HEC-HMS Application to Sen River Catchment in Cambodia. The 7th International Conference on Sustainable Built Environment, February 2018, 0–6.

[18] Clausen, T. J. (2009). Cambodia : Preparing the water resources management (Sector) Project. In Asian Development Bank (Issue September).

[19] Chung, S., Takeuchi, J., Fujihara, M., & Oeurng, C. (2019). Flood damage assessment on rice crop in the Stung Sen River Basin of Cambodia. Paddy and Water Environment, 0123456789.

[20] Neitsch, S. ., Arnold, J. ., Kiniry, J. ., & Williams, J. . (2011). Soil & Water Assessment Tool Theoretical Documentation Version 2009. Texas Water Resources Institute, 1–647.

[21] Al-Qaisi, A. Z., & Al-Shammari, M. J. (2018). Calculation of Water Demand for Multiple Uses in a Specified Region Using a SWAT Model. IOP Conference Series: Materials Science and Engineering, 433(1).

[22] Wei, X., Bailey, R. T., & Tasdighi, A. (2018). Using the SWAT model in intensively managed irrigated watersheds: Model modification and application. Journal of Hydrologic Engineering, 23(10).

[23] Dechmi, F., Burguete, J., & Skhiri, A. (2012). SWAT application in intensive irrigation systems: Model modification, calibration and validation. Journal of Hydrology, 470–471, 227–238.

[24] Ficklin, D. L., Luo, Y., Luedeling, E., & Zhang, M. (2009). Climate change sensitivity assessment of a highly agricultural watershed using SWAT. Journal of Hydrology, 374(1–2), 16–29.

[25] Mishra, P., Singh, U., & Pandey, C. M. (2019). Application of Student' s t - test, Analysis of Variance , and Covariance. 407–411.

[26] Arnold, J. G., Moriasi, D. N., Gassman, P. W., Abbaspour, K. C., White, M. J., Srinivasan, R., Santhi, C., Harmel, R. D., Van Griensven, A., Van Liew, M. W., Kannan, N., & Jha, M. K. (2012). SWAT: Model use, calibration, and validation. Transactions of the ASABE, 55(4), 1491–1508.

[27] R ichter, B. D., Baumgartner, J. V., Braun, D. P., & Powell, J. (1998). A spatial assessment of hydrologic alteration within a river network. River Research and Applications, 14(4), 329–340.

[28] Congalton, R. G. (1991). A review of assessing the accuracy of classifications of remotely sensed data. Remote Sensing of Environment, 37(1), 35–46.

[29] Story, M., & Congalton, R. G. (1986). Remote Sensing Brief Accuracy Assessment: A User's Perspective. Photogrammetric Engineering and Remote Sensing, 52(3), 397–399.

[30] Nelson, R. F. (1983). Detecting Forest Canopy Change Due To Insect Activity Using Landsat Mss. Photogrammetric Engineering and Remote Sensing, 49(9), 1303–1314.

[31] Rosenfield, G. H., & Fitzpatrick-Lins, K. (1986). A coefficient of agreement as a measure of thematic classification accuracy. Photogrammetric Engineering & Remote Sensing, 52(2), 223–227.

[32] Kunthea Nuon. (2005). Soil Map of the lower Mekong Basin. Mekong River Commission. Retrieved from http://archive.iwlearn.net/mrcmekong.org/spatial/meta_html/soil.htm

[33] Neef, A., Touch, S., & Chiengthong, J. (2013). The Politics and Ethics of Land Concessions in Rural Cambodia. Journal of Agricultural and Environmental Ethics, 26(6), 1085–1103.

[34] Bruijnzeel, L. A. (1989). (DE)Forestation and dry season flow in the tropics: A closer look. Tropical Forest Science, 1(3), 229–243. Retrieved from https://www.jstor.org/stable/43594578.

[35] Oliveira, R. S., Bezerra, L., Davidson, E. A., Pinto, F., Klink, C. A., Nepstad, D. C., & Moreira, A. (2005). Deep root function in soil water dynamics in cerrado savannas of central Brazil. Functional Ecology, 19(4), 574–581.

[36] Davis, K. F., Yu, K., Rulli, M. C., Pichdara, L., & D'Odorico, P. (2015). Accelerated deforestation driven by large-scale land acquisitions in Cambodia. Nature Geoscience, 8(10), 772–775.

[37] Kong, R., Diepart, J. C., Castella, J. C., Lestrelin, G., Tivet, F., Belmain, E., & Bégué, A. (2019). Understanding the drivers of deforestation and agricultural transformations in the Northwestern uplands of Cambodia. Applied Geography, 102(April 2018), 84–98. Retrieved from https://doi.org/10.1016/j.apgeog.2018.12.006

[38] Song, L., Boithias, L., Sengtaheuanghoung, O., Oeurng, C., Valentin, C., Souksavath, B., Sounyafong, P., de Rouw, A., Soulileuth, B., Silvera, N., Lattanavongkot, B., Pierret, A., & Ribolzi, O. (2020). Understory limits surface runoff and soil loss in teak tree plantations of Northern Lao PDR. Water (Switzerland), 12(9), 1–23.

[39] Kata Wagner, Akim Kress, T. H. (2021). Forest and Water. Food and Agriculture Organizaion of the United Nations. Retrieved from https://www.fao.org/sustainable-forest-management/toolbox/modules/forest-and water/credits/ru/